Effect of Addition of CeO_2 on Dry Sliding Wear Performance of HVOF Sprayed WC-12Co Coating on Laser Textured AZ91D Alloy

Sachpreet Singh Aulakh[a], Gagandeep Kaushal[b,*], Neeraj Bala[c]

[a]*Research Scholar, Department of Mechanical Engineering, Punjab Technical University, Punjab, India*
[b]*Assistant Professor, Yadavindra College of Engineering, Punjabi University Guru Kashi Campus, Talwandi Sabo, Bathinda, Punjab, India*
[c]*Associate Professor, Mechanical Engineering Department, BBSBEC, Fatehgarh Sahib, Punjab, India*

Abstract

Magnesium alloys are one of the lightest metallic structural materials having high specific strength, good damping, good heat dissipation ability and good electromagnetic shield however wear behavior of these alloys is generally poor. HVOF sprayed WC-Co coatings have been successful used against wear for steel and aluminum alloys. Performance of HVOF coatings depend greatly on the bonding between the coating and the substrate material and surface preparation of magnesium alloys using commonly used surface preparation techniques like grit blasting is fraught with limitations. Rare earth metals have been called as vitamins of materials, which can significantly enhance or alter the properties of materials. This study evaluates the effect of addition of 1% CeO_2 on dry sliding wear performance of HVOF sprayed WC-12Co coatings on laser textured AZ91D alloy. Scanning Electron Microscopy (SEM) and X-ray Diffraction (XRD) techniques have been used to study the morphology of laser textured AZ91D alloy and microstructure of the coatings. Pin on disc dry sliding wear tests were conducted to determine the effect of CeO_2 on wear performance of WC-12Co coatings. The study demonstrates the use of laser texturing as surface preparation method for HVOF WC-Co coatings on AZ91D alloy for wear applications. The addition of 1% CeO_2 seems to protect WC grains from decarburization and grain refinement has been observed in the coating containing cerium. Enhancement of mechanical properties due to lesser decarburization and grain refinement can be attributed to the observed better wear performance of the WC-12Co coatingcontaining CeO_2.

Keywords: Electrical Discharge Machining, Composite Tool, Microstructure, Scanning Electron Microscope.

1. Introduction

Today the biggest challenge facing humanity is to protect the planet from global warming. One of the ways to make an impact in reducing harmful greenhouse gases is through the emissions from automobile, aviation and aerospace sectors. The use of light alloys in the construction of above mentioned sectors can pave the way for lesser greenhouse emissions by reducing weight and consequently, saving energy. Magnesium alloys are one of the lightest metallic structural materials having high specific strength, good damping, good heat dissipation ability and good electromagnetic shield and thus are being increasingly used in aerospace, transportation, civil and military applications [1]. Magnesium alloy has been used in the construction of several automotive and machine parts such as crankcase, camshaft sprocket, gearbox casing, covers, steering column, oil pan, fuel tank barrier and air bag housing etc. [1, 2]. In spite of the fact that in specific applications magnesium alloys have adequate surface properties yet the wear and corrosion behavior of magnesium alloys is commonly poor [3]. Therefore, improvement in wear and corrosion resistance of these alloys would broaden the scope of its applications. The use of coatings can be very effective in protecting magnesium alloys against wear and corrosion.

Magnesium and its alloy have high oxidation susceptibility and it is prone to corrosion in humid environments. Due to this, these materials normally require a complex and therefore an expensive process chain to provide a good coating adherence [4]. In the light of the above discussion, it can be deduced that an alternative substrate surface preparation method prior to thermal spray coating need to be developed to improve the coating adhesion, and hence, coating performance on magnesium alloys and it can widen its area of applications.

Laser techniques like laser texturing and laser ablation as surface treatment methods have been gaining popularity due to advances in laser technology, and advantages associated with it, such as, integration of surface preparation and spray coating, minimal chance of recontamination of surface, faster processing, better process control [5]. In this study laser texturing has been used as surface preparation method to prepare the

*Corresponding Author
Email address: gagankaushal@pbi.ac.in (Gagandeep Kaushal)

AZ91D alloy surface before HVOF coating deposition for good coating adhesion.

High velocity oxy-fuel (HVOF) thermal spray coatings are well known for its ability to produce quality coatings along with high process efficiency. Carbide cermets such as, WC-Co, WC-NiCr and Cr2C3-NiCr have been generally used to produce protection coatings against wear. To enhance the corrosion behavior and mechanical characteristics of the surfaces under such applications, cermets have been widely applied for applications on aluminum alloys [6–8]. The properties of cermet coatings sprayed using HVOF process depend on phase composition, microstructure, grain size, mechanical properties and chemical reactivity to environmental elements. A lot of research has been conducted to see the effect of these factors on the wear and corrosion performance of the coatings [9–11]. Doping with CeO_2 has been found to be beneficial for refinement in grains and uniformity in microstructure in WC-Ni coatings [12–14]. It seems worthwhile to explore the use of CeO_2 in WC-Co coatings for AZ91D alloy for better wear and corrosion performance.

In the context of arguments presented in the earlier section, this research work was undertaken to explore the use of laser texturing as surface preparation method and to see the effect of CeO_2 doping on wear performance of HVOF sprayed WC-12Co coating.

2. Experimental Procedures

2.1. Material

The substrate material used in this study was magnesium alloy AZ91D (Al 8.4%, Zn 3.2%, Mn 0.04%, Cu 0.03%, Fe 0.02%). The substrate was machined into cylindrical shape Φ25.4 mm and length 38.1 mm as per ASTM633C standard and for pin on disc wear testing, cylindrical pins of dimensions Φ 8 mm and length 30 mm were prepared.

2.2. Laser texturing

Laser texturing has been realized on Nd:YAG Q switch laser system. The laser characteristics used are pulse repetition rate 2 KHz, pulse wave duration 100 ns and average power 20 W. A pattern consisting of matrix of holes, with hole-to-hole distance of 100 μm was used to create texture. The scanner stops the laser beam at the points given in drawing and multiple pulses are generated for given duration to create the holes. Helium gas has been used as shroud gas to protect the surface from excessive oxidation.

2.3. HVOF spray parameters

HVOF thermal spray coating technique was used to coat WC-12Co and WC-12Co-1CeO_2 on laser textured AZ91D samples. HVOF technique was used for thermal spray coating because in HVOF technique particles strike the laser textured holes at high velocity as well as in plasticized state due to high temperature of spray particles. Commercial agglomerated and sintered WC-12Co Sulzer metco powder with particle size -45+15μm was used for coating. WC-12Co has been chosen for study because of its good wear and corrosion resistance properties. Tocompare the effect of addition of cerium oxide on microstructure, mechanical properties and wear performance 1% CeO_2(by weight) was added into WC-12Co powder using mechanical mixing method. HVOF spray parameters were as given in the Table 1.

Table 1: HVOF spray parameters

Gun	HIPOJET 2700
Spray distance	180 mm
Oxygen Flow rate	260 L.min^{-1}
LPG flow rate	60 L.min^{-1}
Carrier gas- N_2 flow rate	9.4 L.min^{-1}
Air flow rate	550 L.min^{-1}
Powder feed rate	38 g/min

2.4. Characterization

JSM-6510LV scanning electron microscope was used to study the morphology and microstructure of laser textured and grit blasted surfaces and coatings. Energy-dispersive X-ray spectroscopy (EDX) technique was used to study the composition of coating and coating-interface. The phase constitutions of powder and coatings were determined using X-ray diffractometer (XRD) operated at 40 mA, 45 kV. Porosity of the coating was measured at 12 different points using image analysis of optical images of coating cross-section and the average value has been reported. Coating adhesion strength was investigated using ASTM C633 thermal spray coating adhesion test. An average of three tests was taken to find out adhesion strength. Coating micro hardness was measured on polished cross-section of coating using 200 g load and 10 s dwell time using Vickers indenter on Zwick Roell ZHU micro hardness tester. The reported coating values are average of 16 measurements. Coating fracture toughness was measured using indentation method using the following equation [15]; load of 10 Kg and dwell time of 15 s was used.

$$Kc = 0.0079\left(\frac{P}{a^{\frac{3}{2}}}\right) log\left(4.5\frac{a}{c}\right)$$

Where P(N) represents the load applied to the indenter, a (μm) and c (μm) corresponds to half diagonal and crack length of the indentation respectively.

Dry sliding pin on disc wear tests were conducted on a CETR UMT3 tribometer by pin-on-disc wear test method. Hardened EN32 steel with hardness of 80 HRC was used as counter material. Prior to the wear tests, the surface of all the samples was ground to fine finish using emery papers up to 1000 grit. All the wear tests were performed at the sliding speed of 0.33 m/s at applied

force of 10 and 20 N for a sliding distance of 2000 m. Friction coefficient throughout the test was monitored using integrated software with the tribometer. Displacement of the coated specimens in z-axis was measured online using the displacement sensor integrated with the tribometer. Prior to and post tests, the disc and specimens were washed with acetone in ultrasonic bath and then air-dried in order to prevent contamination. Wear debris was also collected at the end of each test cycle so as to reveal useful information about the wear mechanisms involved and the same was analyzed using SEM and EDS to have insights into wear mechanism.

3. Results

3.1. Laser texturing surface preparation

Figure 1 shows the cross-sectional view of sample prepared using HVOF WC-Co coating sprayed on laser textured AZ91D alloy. Micro-holes can be clearly seen to be formed in the alloy. Further, it can be observed that coating is well anchored inside the micro-holes without any delamination. Coating adhesion strength of the coating as measured using ASTM C633 test standard has been found to be 45.60 MPa [16]. No delamination or failure of the coating was observed instead separation of the counter sample happened due to adhesive failure.

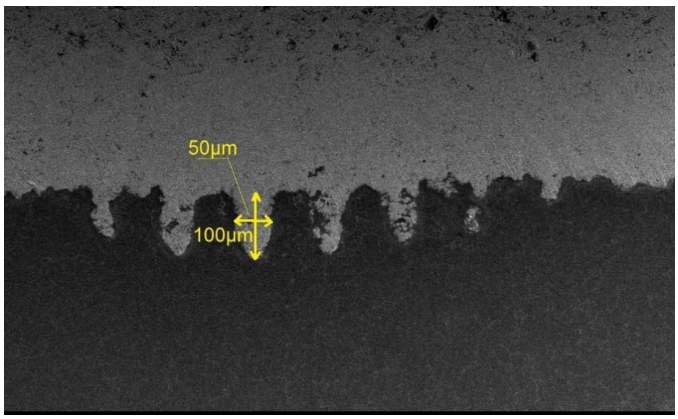

Figure 1: Cross-sectional view of laser textured and coated sample

3.2. Coating characterization

Figure 2 presents comparative XRD analysis between WC-12Co and WC-12Co-1CeO_2 coatings. The XRD pattern of the coating with cerium indicates presence of WC, Co_6W_6C, Co_3W_3C. However, there is no decarburization of WC into W_2C as indicated by XRD pattern. There is significant peak corresponding to α cobalt showing its presence in the coating. The hump in XRD pattern between 2θ of 25° and 40° is also significantly lesser as compared to WC-12Co coating.

Figure 3 shows full width at half maximum (FWHM) values for major WC peaks for WC-12Co and WC-12Co-CeO_2 coatings. The FWHM value at major WC peak at

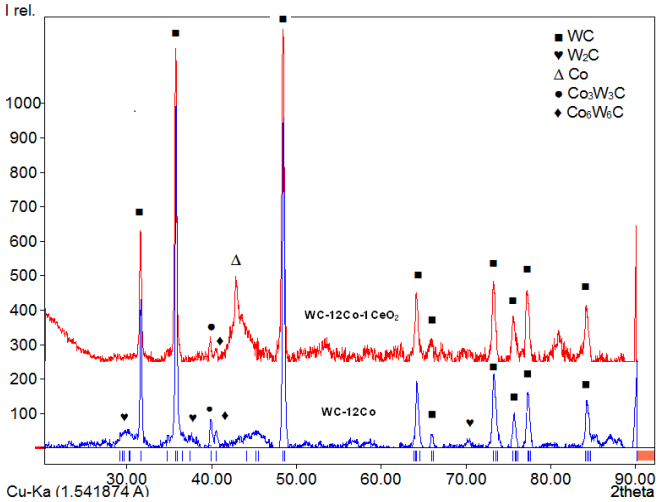

Figure 2: Comparative XRD analysis of WC-12Co & WC-12Co-1CeO_2

35.8°, for the coating with CeO_2 is more than that of the WC-12Co coating. Significance of FWHM and interpretation of these results will be dealt with in the discussion section.

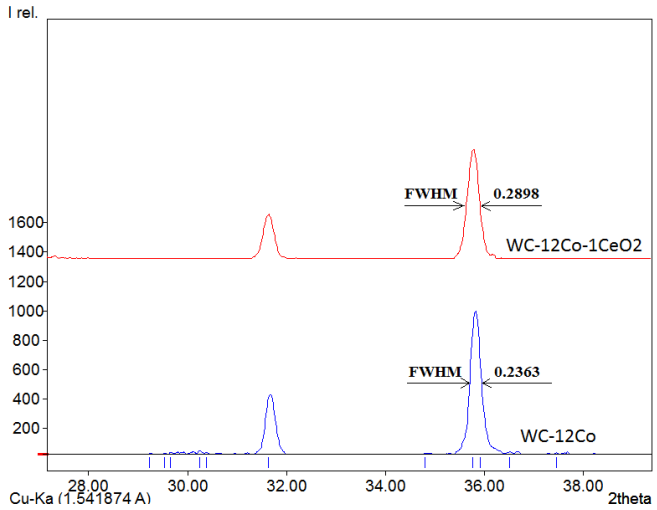

Figure 3: FWHM values of WC-12Co and WC-12Co-CeO_2 coatings

Figure 4 shows the microstructure of as sprayed and polished cross-section of coated samples. It can be seen (Figure 4a) that WC particles in WC-12Co coating have significant amount of white rim around them. It shows decarburization of WC particles into W_2C. However, as per Figure 4c, presence of white rings showing W_2C is not so pronounced in WC-12Co-1 CeO_2 coating. Roundness of the corners in WC particles can be seen in Figure 4b, while in Figure 4d WC particles are having angular corners. Roundness of the corners in WC particles signifies decarburization.

One of the factors to affect the coating's wear resistance is microhardness of the coating. Microhardness

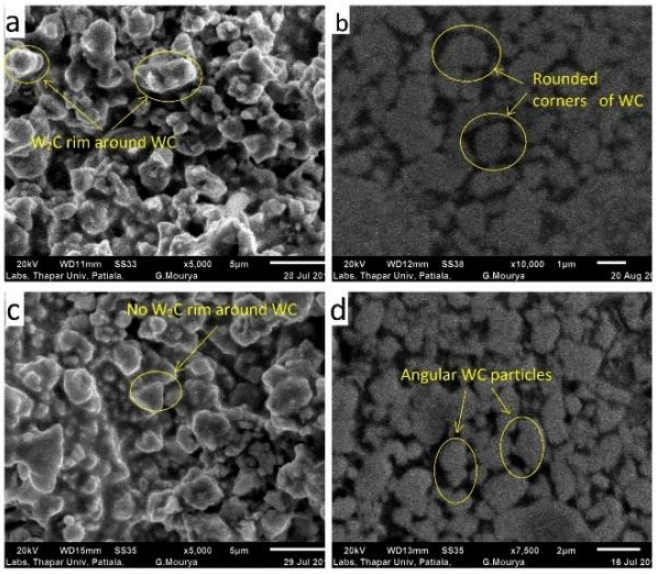

Figure 4: FE-SEM micrographs of coated samples (a) as sprayed WC-12Co (b) polished cross-section ofWC-12Co (c) as sprayed WC-12Co-1CeO_2 (d)polished cross-section of WC-12Co-1CeO_2

of the W-12Co coating is found to be $HV_{0.2}$ 1063.1 ± 121.4 while that of WC-12Co-1CeO_2 coating is $HV_{0.2}$1040.0±110.14. For good wear performance, the coating should have high hardness along with high fracture toughness. These two coating characteristics are not complimentary; if hardness of the coating is high, it generally has low toughness and vice-versa. Fracture toughness of coatings was measured using vicker's hardness indentation method on cross-section with one of the diagonals parallel to interface. The values of toughness obtained from testing are: WC-12Co - 5.95±0.96 MPa $m^{1/2}$, WC-12Co-1-CeO_2 - 7.33±0.19 MPa $m^{1/2}$. Fracture toughness of the coating seem to increase with reducing decarburization and amorphization.

3.3. Dry sliding wear behavior

WC-12Co and WC-12Co-1CeO_2 coatings were sprayed on the surface of AZ91D pins prepared using laser texturing surface preparation method. It was observed during the dry sliding wear testing of coated samples that as compared to WC-12Co coating, WC-12Co-1CeO_2 coating gained weight afterwear test suggesting no or negligible wear of coated samples. The commonly used methods to measure wear rate like, weight loss or volume loss could not be used to quantify wear rate of coatings. Hence, online measurement of displacement of coated sample has been used to observe the wear response of the coated specimen. The dry sliding wear behavior of coated specimens on EN32 counter disc for applied loads of 10 N and 20 N for a sliding distance of 2000 m is as shown in Figure 5a and Figure 5b. It can be seen from Figure 5a and Figure 5b that coatings with Cerium show negative wear, both at 10 N as well as 20 N load. Negative wear is an indication that specimen increased weight with subsequent increase in sample length resulting in the sample being raised from the counter surface. Positive wear for WC-12Co coating indicate that during sliding the sample lost approximately 10 µm of coating. While WC-12Co coating initially indicates positive wear followed by negative wear by gaining height. WC-12Co-1CeO_2 samples show increase in sample length. As compared to the sliding wear behavior at 10 N, gain in length for WC-12Co-1CeO_2 coatings is greater at 20 N load. It can be seen that after gain in length up to a critical value during beginning of the sliding test there is gradual wear loss throughout the test.

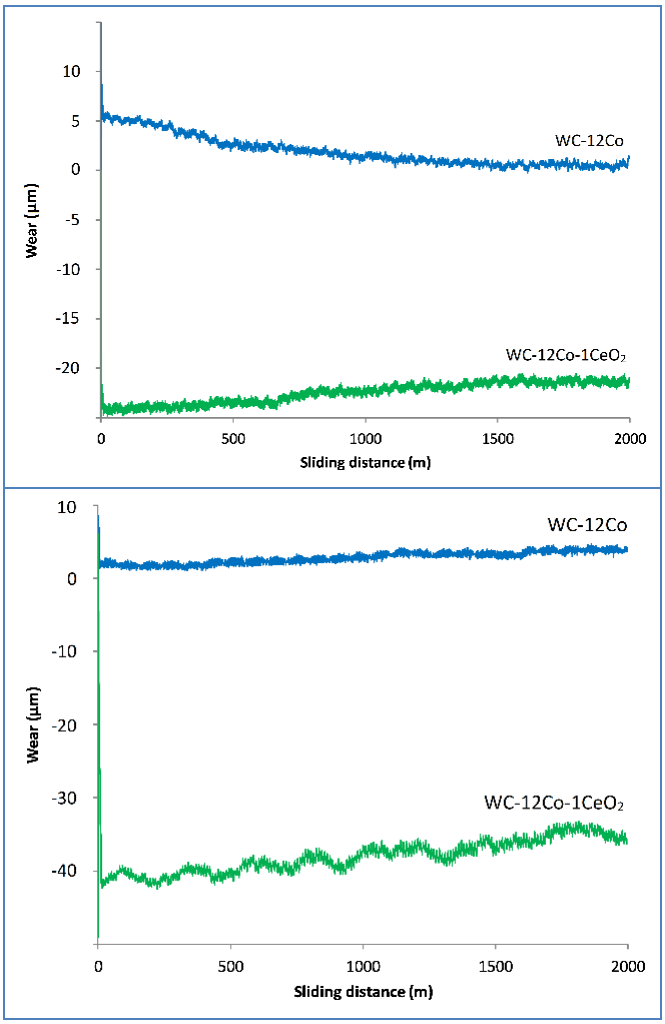

Figure 5: Dry sliding wear behavior of coatings at (a) 10 N applied load (b) 20 N applied load

4. Discussion

XRD analysis (Figure 2) of WC-12Co coating revealed WC, W2C, Co_3W_3C, Co_6W_6C phases. W_2C is the result of decarburization of WC into W_2C and η phases of Co_3W_3C, Co_6W_6C happen when decomposed products of

WC like W_2C and Wdissolve into metallic Co to form amorphous compounds with cobalt. Similarresults have been reported by many researchers [10, 17]. No presence of α cobalt point towards dissolution of W and C into cobalt. However, XRD patterns in the case of WC-12Co coating with cerium did not showany W_2C. The presence of complex carbides is there, but the intensity of thesecarbides is lesser than that for WC-12Co coating. The coating with cerium alsopoints towards presence of α cobalt. The difference in the behaviour of the WC-12Co with cerium is explained by the researchers [12]. They explainthat the CeO_2 particles having high melting point make a heat shield around WC particles by absorbing heat to prevent severe decarburization of WC particles.

Figure 3 shows that FWHM value of WC-12Co coating at 2θ - 35.800 is smaller than the FWHM value of the coating with cerium. As per Scherrer formula [12] quoted here:

$d=K.\lambda/\beta.\mathrm{Cos}(\theta)$

where, d is the grain size, K is constant, λ is wave-length of X-ray, β is full width at half maximum and θ is diffraction angle.

From the formula, it can be deduced that grain size (d) of the major phase decreases as value of FWHM (β) increases, therefore according to FWHM results,it can be said that microstructure of the coating has refined in the coating with cerium. Grain refinement in WC-Co/Ni coatings with the addition of CeO_2 has also been reported earlier by [12, 13, 18] as well.

SEM images (Figure 4) show the microstructure of the coatings. If shape of WC inWC-12Co coating in Figure 4b is compared to the shape of WC in the coating with cerium (Figure 4d), it can be seen that WC particles are more round in shape as compared to that of Figure 4d which are angular. The CeO_2 particles having high melting point make a protective shield around WC particles and save them from severe decarburization Further, more decarburization of WC-12Co coating as compared to the cerium coatings is confirmed by more white colored rims around WC particles in Figure 4a.

It can be observed from the Figure 5a and Figure 5b that the WC-12Co-1CeO_2 coatings display increase in length or weight of pin specimens after sliding wear test. The gain in weight or length of the WC-12Co-1CeO_2 coatings can be explained by the argument that when harder coatings are slid against relatively softer EN32 disc, the disc material suffer wear, because hard WC particles at the surface of coated sample cause plastic deformation of disc material. Wear of disc is even higher for 20 N applied load due to increased penetration of WC particles into disc. Figure 6 shows the proposed wear mechanism at play in the present study. The wear particles are removed from the disc or the coating surface due to combined action of plastic deformation and adhesion with the coating which results into formation of transfer film on coating surface and subsequent increase in length of sample. However, if coating is brittle or has less toughness, during on going sliding coating particles along with attached transfer film breakoff from coating, resulting in decrease in length of sample. Similar mechanism of wear particles generation is proposed by Pirso et al [19] as well.

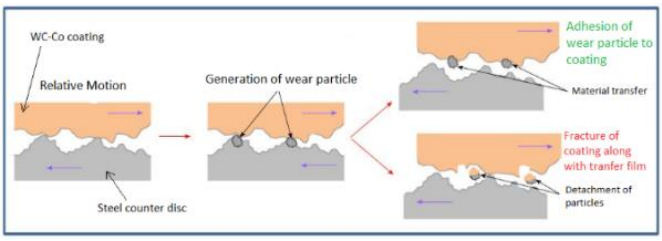

Figure 6: Schematic depicting proposed wear mechanism

Subsequently, worn out particles are converted into fine wear particles by hard asperities of WC. Due to high temperatures generated by friction, these particles join together and reattach themselves to the specimen, whereby forming a transfer film. The transfer film, generated on the surface of coating dramatically reduces wear [20].Inter locking of abraded particles between valleys and hard WC asperities on the surface of coating maintain the transfer film on the surface of coated sample. Wear of the disc surface is more at higher applied load, which generates more wear debris. The lock-in of film particles between hard WC is also greater at higher loads due to greater degree of compacting on the coating surface. Subsequently, thickness of transfer film and hence length gained by specimen is also more at higher applied load. The stability of the transfer-film is reduced as it grows thick. Hence, counter removal of wear debris from transfer film takes place, which keeps the thickness of the film below a critical value.

Thickness of the transfer film is not the same for all the coatings. It is highest forWC-12Co-1CeO_2 coatings and lowest for WC-12Cocoatings. WC-12Co coating has highest decarburization and amorphization as compared to the cerium oxide containing coating. Decarburization of WC into W_2C increases the hardness as well as brittleness of the coating, which may result intosevere wear [12]. However, due to higher brittleness of WC-12Co coating compared to WC-12Co-1CeO_2 coating on account of higher decarburisation, fatigue fracture of coating particles may happen which breaks the transfer film, resulting into more abrasion and hence wear of the coating. Figure 7 shows the SEM micrographs of the worn surface of WC-12Co coating and Figure 8 shows the wear debris. The SEM micrographs conform to the proposed wear mechanism for WC-12Co coating.

Wear resistance of the thermal coating is dependent of many factors including microstructure, hardness and toughness [10, 21]. It has been observed through FWHM values in XRD analysis that grain size of WC is finer in WC-12Co-CeO_2 coating as compared to that of WC-12 Co coating. Decarburisation and amorphisation of

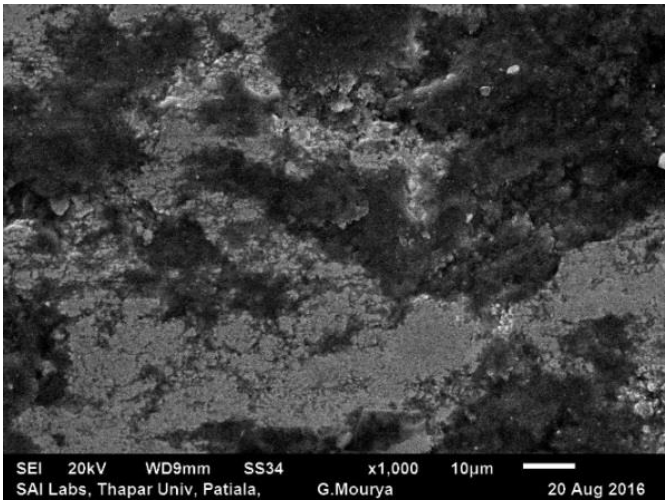

Figure 7: SEM micrograph of the worn surface of WC-12Co coating showing wear damage

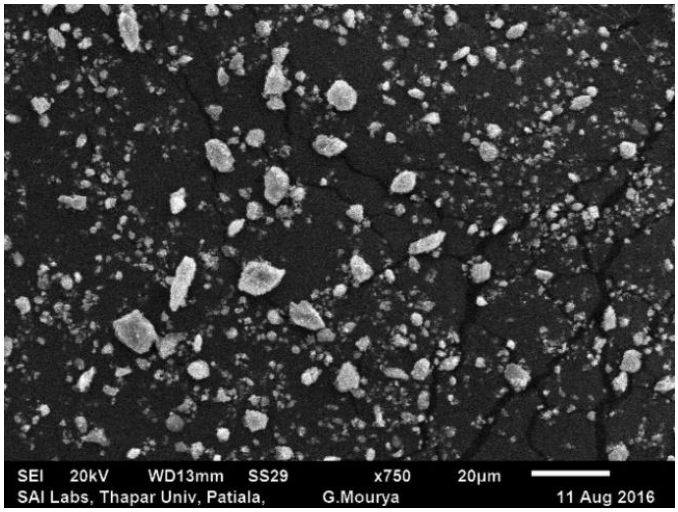

Figure 8: SEM micrograph of debris generated by wear of WC-12Co coating

WC-12Co-1CeO_2 coating has been found to be lesser as compared to WC-12Co coating. Furthermore, presence of ductile α Co has also been observed in WC-12Co-1CeO_2 coating. All these factors increase the fracture toughness and hence strength of the coating. During dry sliding against EN32 counter disc, wear debris from the disc is generated and it forms a transfer film at the surface of the coating. However, unlike WC-12Co coating, the WC-12Co-1CeO_2 coating has high fracture toughness and it prevents fatigue fracture of the coatingparticles. Hence, WC-12Co-1CeO_2 coatings are ableto maintain stable transfer film on the surface of the specimen which prevents wear of the specimen. The mixed metal transfer film can be clearly seen in the Figure 9, which supports the proposed wear mechanism for WC-12Co-1CeO_2 coating. Further, Figure 10 shows EDX analysis of wear debris generated by WC-12Co-1CeO_2 coating. EDX analysis shows presence of Fe,Co and W in the debris particle, indicating that debris originated from transfer film on the surface of coating.

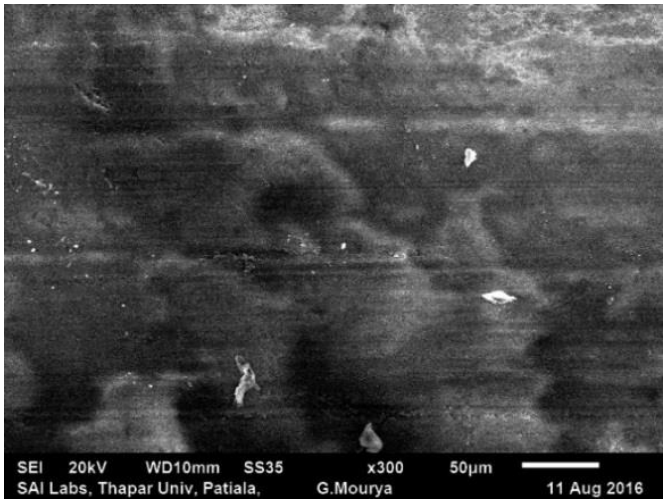

Figure 9: SEM micrograph of worn surface of WC-12Co-1CeO_2 coatings showing mixed metal transfer film

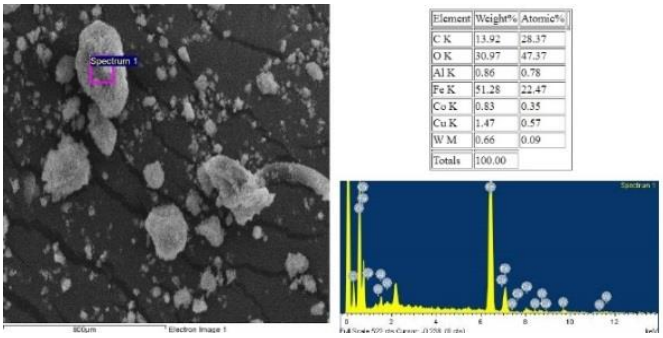

Element	Weight%	Atomic%
C K	13.92	28.37
O K	30.97	47.37
Al K	0.86	0.78
Fe K	51.28	22.47
Co K	0.83	0.35
Cu K	1.47	0.57
W M	0.66	0.09
Totals	100.00	

Figure 10: EDX analysis of debris particle indicating presence of iron

It can be observed from the discussion that, WC-12Co-1CeO_2 coatings have better wear performance in dry sliding wear against EN32 counter surface. The higher wear resistance for these coatings originate from stable mixed metal film formation at the surface, due to higher fracture toughness on account of less decarburisation and amorphisation. However, nostable film formation takes place forWC-12Co coating because of brittle fracture of coating particles during sliding. Hence, it can be concluded that a balance of hardness and toughness is essential for good wear performance of the coating against hardened steel surface and due to this very reason the coating with cerium have better wear resistance.

5. Conclusions

The study aimed to see the effect of addition of CeO_2 on dry sliding wear performance of HVOF sprayed WC-12Co coatings on laser textured AZ91D alloy.

The main findings of the study are as follows,

- Laser texturing can be successfully used to create micro texture on the surface of AZ91D alloy and the HVOF WC-Co coatings deposited on the laser textured surface achieve high bond strength.
- SEM microstructure analysis of the as sprayed and cross-sectioned samples indicates towards lesser decarburization of WC in the coating with CeO_2.
- XRD analysis of coatings points to higher FWHM value for the coating with CeO_2. Higher value of FWHM is an indication of grain refinement.
- Pin on disc sliding wear performance testing reveals better wear performance for the coating with CeO_2. As compared to positive wear observed in WC-12Co coating, the WC-12CO-1CeO_2 coating have shown negative wear. The pin samples prepared using WC-12CO-1CeO_2 coating gained length, which can be attributed to mixed metal transfer film made up of wear particles from steel disc.
- Better wear performance of the cerium containing coating can be said to be due to its higher toughness on account of low decarburization and grain refinement effect.

References

[1] K. U. Kainer, B. L. Mordike, Magnesium alloys and their applications, Wiley-VCH Weinheim, 2000.

[2] A. Luo, Magnesium technology: Proceedings of tms annual meeting, Charlotte, North Carolina, USA.

[3] K. Spencer, D. Fabijanic, M.-X. Zhang, The use of al–al2o3 cold spray coatings to improve the surface properties of magnesium alloys, Surface and Coatings Technology 204 (3) (2009) 336–344.

[4] M. Parco, L. Zhao, J. Zwick, K. Bobzin, E. Lugscheider, Investigation of hvof spraying on magnesium alloys, Surface and Coatings Technology 201 (6) (2006) 3269–3274.

[5] N. Serres, F. Strasbourg, S. Costil, A. Lamraoui, C. Langlade, C. Coddet, Life cycle assessment of surface preparation processes implemented before thermal spray, International Thermal Spray Conference and Exposition 276 (2011) 1–5.

[6] M. Magnani, P. Suegama, N. Espallargas, S. Dosta, C. S. Fugivara, J. Guilemany, A. V. Benedetti, Influence of hvof parameters on the corrosion and wear resistance of wc-co coatings sprayed on aa7050 t7, Surface and Coatings Technology 202 (19) (2008) 4746–4757.

[7] M. Barletta, G. Bolelli, B. Bonferroni, L. Lusvarghi, Wear and corrosion behavior of hvof-sprayed wc-cocr coatings on al alloys, Journal of Thermal Spray Technology 19 (1) (2010) 358–367.

[8] H. Mindivan, Wear behavior of plasma and hvof sprayed wc-12co+ 6% etfe coatings on aa2024-t6 aluminum alloy, Surface and Coatings Technology 204 (12-13) (2010) 1870–1874.

[9] A. Lekatou, D. Sioulas, A. Karantzalis, D. Grimanelis, A comparative study on the microstructure and surface property evaluation of coatings produced from nanostructured and conventional wc–co powders hvof-sprayed on al7075, Surface and Coatings Technology 276 (2015) 539–556.

[10] M. Xie, S. Zhang, M. Li, Comparative investigation on hvof sprayed carbide-based coatings, Applied Surface Science 273 (2013) 799–805.

[11] A. Basak, J.-P. Celis, P. Ponthiaux, F. Wenger, M. Vardavoulias, P. Matteazzi, Effect of nanostructuring and al alloying on corrosion behaviour of thermal sprayed wc–co coatings, Materials Science and Engineering: A 558 (2012) 377–385.

[12] L. He, Y. Tan, H. Tan, Y. Tu, Z. Zhang, Microstructure and tribological properties of wc-ceo2/ni-base alloy composite coatings, Rare Metal Materials and Engineering 43 (4) (2014) 823–829.

[13] M. M. Sharma, T. J. Eden, B. T. Golesich, Effect of surface preparation on the microstructure, adhesion, and tensile properties of cold-sprayed aluminum coatings on aa2024 substrates, Journal of Thermal Spray Technology 24 (3) (2015) 410–422.

[14] Y. Wang, Q. Zhang, M. Su, Q. Zhong, The influence of ceo 2 on the corrosion resistance of laser remelted alloy spray coatings on steel, Scripta metallurgica et materialia 32 (6) (1995) 891–894.

[15] A. Evans, T. R. Wilshaw, Quasi-static solid particle damage in brittle solids—i. observations analysis and implications, Acta Metallurgica 24 (10) (1976) 939–956.

[16] S. Aulakh, G. Kaushal, Laser texturing as an alternative to grit blasting for improved coating adhesion on az91d magnesium alloy, Transactions of the IMF 97 (2) (2019) 100–108.

[17] M. Couto, S. Dosta, J. Guilemany, Comparison of the mechanical and electrochemical properties of wc-17 and 12co coatings onto al7075-t6 obtained by high velocity oxy-fuel and cold gas spraying, Surface and Coatings Technology 268 (2015) 180–189.

[18] Y. Liu, Z. Hang, G. Yang, H. Fu, N. Xi, H. Chen, Influence of rare earth on the high-temperature sliding wear behavior of wc-12co coating prepared by hvof spraying, Journal of Thermal Spray Technology 27 (7) (2018) 1143–1152.

[19] J. Pirso, M. Viljus, S. Letunovitš, Friction and dry sliding wear behaviour of cermets, Wear 260 (7-8) (2006) 815–824.

[20] V. Rajinikanth, K. Venkateswarlu, An investigation of sliding wear behaviour of wc–co coating, Tribology International 44 (12) (2011) 1711–1719.

[21] E. Celik, O. Culha, B. Uyulgan, N. A. Azem, I. Ozdemir, A. Turk, Assessment of microstructural and mechanical properties of hvof sprayed wc-based cermet coatings for a roller cylinder, Surface and Coatings Technology 200 (14-15) (2006) 4320–4328.